Monthly Notices
of the
ROYAL ASTRONOMICAL SOCIETY

Mon. Not. R. Astron. Soc. **415,** 2827–2831 (2011) doi:10.1111/j.1365-2966.2011.18901.x

Constraining the star formation rate in the solar neighbourhood with star clusters

C. Bonatto★ and E. Bica

Departamento de Astronomia, Universidade Federal do Rio Grande do Sul, Av. Bento Gonçalves 9500, Porto Alegre 91501-970, RS, Brazil

Accepted 2011 April 11. Received 2011 April 11; in original form 2011 March 1

ABSTRACT

This paper investigates the star formation rate (SFR) in the solar neighbourhood. First, we build the local age distribution function (ADF) with an updated sample of 442 star clusters located at less than 1 kpc from the Sun. Next, we define the SFR, compute the individual mass evolution of a population of artificial clusters covering the broad range of parameters observed in actual clusters, and assume $100\,M_\odot$ as the low-mass limit for effective cluster observation. This leads to a simulated ADF, which is compared to the low-noise solar neighbourhood ADF. The best match corresponds to a non-constant SFR presenting two conspicuous excesses for ages $\leq$9 Myr and between 220–600 Myr (the local starburst). The average SFR is $\overline{\mathrm{SFR}} \approx (2500 \pm 500)\,M_\odot\,\mathrm{Myr}^{-1}$, corresponding to the average surface SFR $\overline{\Sigma}_{\mathrm{SFR}} \approx (790 \pm 160)\,M_\odot\,\mathrm{Myr}^{-1}\,\mathrm{kpc}^{-2}$. These values are consistent with the SFR inferred from embedded clusters (ECs), but much lower ($\lesssim$16 per cent) than that implied by field stars. Both the local starburst and the recent star formation period require SFR $\sim 2 \times \overline{\mathrm{SFR}}$ to be described. The simulations show that 91.2 ± 2.7 per cent of the clusters created in the solar neighbourhood do not survive the first 10 Myr, which is consistent with the rate of EC dissolution.

Key words: open clusters and associations: general.

1 INTRODUCTION

It is currently accepted that star formation is scale-free and hierarchical, with high-velocity turbulent gas forming large-scale structures, while low-velocity compression forms small clumps (Elmegreen 2008). A natural consequence of this scenario is that young stellar groupings would be hierarchically clustered, with the great star complexes at the largest scales and the OB associations and subgroups, clusters and cluster subclumps, at the smallest (e.g. Efremov 1995). The bottom line is that star formation appears to occur primarily in clusters. Consequently, star clusters appear to be excellent tracers of the star formation rate (SFR) and history of the Galaxy, provided that their fundamental parameters – especially the age – are known.

However, star clusters have limited lifetimes. At the earliest phases, most of the embedded star clusters (ECs) dissolve into the field on a time-scale of a few 10^7 Myr. Dissolution here occurs mainly because the gravitational potential can be rapidly reduced by the impulsive gas removal by supernovae and massive star winds associated with this early period. Thus, a significant fraction of the stars, especially of low mass, end up moving faster than the scaled-down escape velocity, and may escape into the field (e.g. Goodwin & Bastian 2006).

Dissolution also affects the open clusters (OCs) that survive the early phase. Even around the solar circle, most OCs dissolve long before reaching an age of $\sim$1 Gyr (e.g. Bonatto et al. 2006). The disruption time-scale, in general, scales with mass as $t_{\mathrm{dis}} \sim M^{0.62}$ (e.g. Lamers & Gieles 2006), which means that solar neighbourhood clusters with mass in the range 10^2– $10^3\,M_\odot$ dissolve on a time-scale $75 \lesssim t_{\mathrm{dis}}(\mathrm{Myr}) \lesssim 300$. This occurs because OCs continually undergo mass segregation and evaporation, tidal interactions with Galactic substructures, shocks with giant molecular clouds (GMCs), as well as mass-loss due to stellar evolution. By decreasing the total cluster mass and the collective gravitational potential, these processes affect the internal dynamics and accelerate the cluster dynamical evolution. Eventually, the majority of the OCs dissolve in the Galactic stellar field.

Thus, the only way of recovering the SFR using the observed star cluster population is by taking the mass-loss processes affecting clusters of different masses and orbits into account. To this effect, semianalytical descriptions of the main mass-loss processes have become available recently (e.g. Khalisi, Amaro-Seoane & Spurzem 2007; Lamers, Baumgardt & Gieles 2010). In this paper, we employ these processes to simulate the mass evolution of a population of artificial clusters. Properties of the local SFR are then derived by

★E-mail: charles@if.ufrgs.br

comparing the simulated age distribution function (ADF) with that built for clusters in the solar neighbourhood.

This paper is organized as follows. In Section 2, we build the ADF for the solar neighbourhood. In Section 3, we briefly discuss the cluster mass-loss process. In Section 4, we simulate the observed ADF and use it to constrain the local SFR. Concluding remarks are given in Section 5.

2 BUILDING THE OBSERVED CLUSTER ADF

The number of star clusters with accurate age and distance determinations has been steadily increasing over the last years. This is particularly true for the very young clusters, most of which so embedded in their parent gas and dust cloud that their stellar content is essentially inaccessible to optical photometry. However, the availability of uniform, wide-field and rather deep near-infrared surveys (e.g. 2MASS,[1] GLIMPSE[2]), and some covering essentially all the sky (2MASS) has led to the discovery – and allowed a robust parameter derivation – of many such ECs (e.g. Bica et al. 2003; Dutra et al. 2003; Kumar, Kamath & Davis 2004; Bonatto, Santos & Bica 2006; Kumar, Keto & Clerkin 2006; Ortolani et al. 2008; Bonatto & Bica 2009b,c, 2010a), together with some old and/or very reddened OCs (e.g. Bonatto & Bica 2007, 2008; Froebrich, Scholz & Raftery 2007; Bonatto & Bica 2009a, 2010b; Froebrich et al. 2010).

Together with the several hundred objects already indexed in the widely used star cluster data bases, WEBDA[3] and DAML02,[4] the recent discoveries (together with the parameter derivation for poorly studied and/or unstudied objects) are proving invaluable in constructing a more detailed picture of the cluster ADF, especially in the solar neighbourhood and for very young clusters (Section 4).

We started by searching WEBDA and DAML02 for clusters with the available age ($t_{\rm A}$) and distance from the Sun ($d_\odot$). However, given the amount of new data routinely published, it usually takes a considerable time for both data bases to incorporate the recently discovered clusters, or to update previous entries with newly derived parameters. Then, we complemented the sample by searching the recent literature for clusters that still are not listed in either data base. Cluster designations and coordinates have been checked in all sources (WEBDA, DAML02, and the literature) to avoid duplicity. When multiple values of age and/or distance occurred, we adopted those based on colour–magnitude diagrams, or the more recent. The final sample contains 1718 clusters (ECs and OCs) with age and distance, of which 442 are closer than 1 kpc from the Sun.[5] By far, most of the parameters have been taken from WEBDA and DAML02, which do not provide measurement uncertainties. Thus, based on our experience in working with clusters of different ages and distances, we adopted the following uniform error attribution: 10 per cent for $d_\odot < 1$ kpc, 15 per cent for $1 < d_\odot$ (kpc) < 5, 20 per cent for $5 < d_\odot$ (kpc) < 9 and 25 per cent for $d_\odot > 9$ kpc; 35 per cent for $t_{\rm A} < 20$ Myr, 30 per cent for $20 < t_{\rm A}$(Myr) < 100, 20 per cent for $100 < t_{\rm A}$(Myr) < 2000 and 50 per cent for $t_{\rm A} > 2000$ Myr.

Age uncertainties are explicitly incorporated into the ADF, which is defined as the fractional number of clusters *per* Myr, ADF $\equiv {\rm d}N/{\rm d}t_{\rm A}$. Formally, if measurements of a given parameter χ are normally (i.e. Gaussian) distributed around the average $\bar{\chi}$ with a standard deviation σ, the probability of finding it at a specific value χ is given by $P(\chi) = \frac{1}{\sqrt{2\pi}\sigma} {\rm e}^{-\frac{1}{2}(\frac{\chi-\bar{\chi}}{\sigma})^2}$. To build this ADF, we first define a set of bins spanning the whole range of ages and having widths that increase with age (to account for the decreasing number of clusters at older ages). Then, for a cluster with age and uncertainty $t_{\rm A} \pm \sigma$, we compute the probability that the age corresponds to a given bin, which is simply the difference between the error functions at the bin borders. By doing this for all clusters and age bins, we have the number density of clusters in each age bin. By definition, the integral of the ADF over the whole range of ages is the number of clusters. Subsequently, bin widths can be adjusted to minimize the errors, so that the resulting ADF has statistically meaningful values over all ages.

3 OVERVIEW OF THE MASS-LOSS PROCESSES

Star clusters lose mass continually by a combination of processes associated with stellar evolution and dynamical interactions (both internal and external to the cluster). Robust analytical descriptions of the mass-loss processes – for clusters characterized by a wide variety of parameters and orbiting in different environments – have become available in recent years, with model parameters derived from theoretical grounds (e.g. Spitzer 1987; Lamers et al. 2010) and N-body simulations (e.g. Baumgardt & Makino 2003; Gieles & Baumgardt 2008). Formally, the time-rate of the change in the mass of a cluster that was formed with the mass $M_{\rm i} = M(0)$ can be expressed as

$$\frac{{\rm d}M}{{\rm d}t} = \sum_{p=1}^{6} \left(\frac{{\rm d}M}{{\rm d}t}\right)_p , \qquad (1)$$

where the mass-loss processes p are (1) stellar evolution; (2) tidal effects by a steady field; (3) shocks with spiral arms; (4) encounters with GMCs; (5) evaporation; and (6) ejection. For processes (1)–(4), we adopt the semianalytical approach of Lamers & Gieles (2006) and Lamers et al. (2010). In what follows, we assume that masses are always expressed in solar masses ($M_\odot$) and time in Myr; also, we write the equations in terms of the remaining-mass fraction $\mu \equiv M/M_{\rm i}$. For clarity, we provide below a brief description of these processes.

3.1 Stellar evolution

Since we are dealing essentially with disc clusters, we adopt the solar metallicity approximation given by Lamers & Gieles (2006), which is based on single stellar population GALEV models (Anders & Fritze-v. Alvensleben 2003) and a Salpeter-like (Salpeter 1955) mass function:

$$\left(\frac{{\rm d}\mu}{{\rm d}t}\right)_{\rm se} = -\mu \left(\frac{a}{t}\right) 10^{[(a-1)\log(qq)+qq^a+b]},$$

with $qq = \log(t) - 1.0$, $a = 0.255$ and $b = -1.805$. This process is relevant for $t > 10$ Myr.

[1] The Two-Micron All-Sky Survey, All Sky data release (Skrutskie et al. 2006).

[2] Galactic Legacy Infrared Mid-Plane Survey Extraordinaire (Benjamin et al. 2003).

[3] www.univie.ac.at/webda

[4] Catalog of Optically Visible Open Clusters and Candidates (Dias et al. 2002).

[5] Upon request, the table with the age and distance from the Sun for the 442 nearby clusters is available from one of us (CB).

3.2 Tidal effects

We adopt the semianalytical description of the mass-loss of clusters on a steady tidal field of Lamers et al. (2010), which is expected to apply to a broad range of cluster conditions and orbit environments:

$$\left(\frac{\mathrm{d}\mu}{\mathrm{d}t}\right)_{\mathrm{tidal}} = -\frac{\mu^{1-\gamma}}{t_{\mathrm{o}} M_{\mathrm{i}}^{\gamma}},$$

with $t_{\mathrm{o}} = t_R(\frac{1-\epsilon}{\bar{m}^{\gamma}})(\frac{R_{\mathrm{G}}}{8.5\,\mathrm{kpc}})(\frac{v_{\mathrm{G}}}{220\,\mathrm{km\,s^{-1}}})^{-1}$, where $t_R = 13.3$ Myr for clusters with an initial concentration factor of the density King profile $W_0 = 5$ and $t_R = 3.5$ Myr for $W_0 = 7$; $\gamma = 0.65$ for $W_0 = 5$ and $\gamma = 0.8$ for $W_0 = 7$; thus, both γ and t_R are not independent parameters, since they can be expressed as a function of W_0; ϵ is the cluster orbit eccentricity; the average stellar mass at time t is given by the interpolation formula $\bar{m}(t) = 0.6193 - 0.0362\tau - 0.014\,81\tau^2 + 0.0022\tau^3$, where $\tau = \log(t)$; R_{G} is the cluster's Galactocentric distance and v_{G} is the (assumed constant) rotation velocity. In what follows, we take $v_{\mathrm{G}} = 200\,\mathrm{km\,s^{-1}}$ for orbits around the solar neighbourhood.

3.3 Shocks with spiral arms

The energy gain and the mass-loss due to the disruptive effect of spiral-arm passages of star clusters with planar and circular orbits around the centres of galaxies have been thoroughly studied by Gieles, Athanassoula & Portegies Zwart (2007). In particular, for the solar neighbourhood, Gieles et al. (2007) and Lamers & Gieles (2006) find

$$\left(\frac{\mathrm{d}\mu}{\mathrm{d}t}\right)_{\mathrm{sp}} = -5\times10^{-5}\frac{\mu^{0.3}}{(M_{\mathrm{i}}/10^4\,\mathrm{M}_{\odot})^{0.7}}.$$

3.4 Encounters with GMCs

Similarly to the spiral arms, Lamers & Gieles (2006) estimate the energy gain and mass-loss due to encounters between clusters and GMCs. Assuming GMC parameters typical of the solar neighbourhood, they find

$$\left(\frac{\mathrm{d}\mu}{\mathrm{d}t}\right)_{\mathrm{GMC}} = -5\times10^{-4}\frac{\mu^{0.3}}{(M_{\mathrm{i}}/10^4\,\mathrm{M}_{\odot})^{0.7}}.$$

The mass-loss due to GMCs is thus 10 times higher than that of the spiral arms.

3.5 Ejection and evaporation

Stars can also escape from a cluster by means of ejection and evaporation. Ejection occurs when, after a single, close encounter with another star, a member ends up with excess velocity with respect to the escape velocity. Evaporation, on the other hand, is related to a series of more distant encounters that gradually increase a star's energy, eventually leading it to escape from the cluster. With the respective time-scales taken from Khalisi et al. (2007, and references therein), the mass-loss associated with both processes are, respectively,

$$\left(\frac{\mathrm{d}\mu}{\mathrm{d}t}\right)_{\mathrm{ej}} = -\frac{\bar{m}(G\mu)^{1/2}}{46\left(M_{\mathrm{i}}R_{\mathrm{hm}}^3\right)^{1/2}}$$

and

$$\left(\frac{\mathrm{d}\mu}{\mathrm{d}t}\right)_{\mathrm{ev}} = -\frac{\bar{m}(G\mu)^{1/2}\ln(\gamma_{\mathrm{c}}N)}{13.8\left(M_{\mathrm{i}}R_{\mathrm{hm}}^3\right)^{1/2}},$$

where the half-mass radius is given by $R_{\mathrm{hm}} = 3.75(M/10^4)^{0.1}$ (Larsen 2004), $\gamma_{\mathrm{c}} = 0.11$ is the Coulomb factor, $N = M(t)/\bar{m}(t)$ is the number of stars at time t and G is the gravitational constant.

3.6 The adopted procedure

In summary, given a cluster of the initial mass M_{i}, and a set of model parameters (R_{GC}, W_0, γ, ϵ, t_R), equation (1) should be solved to find the mass still bound to the cluster at a later time t, $M = M(t)$.

4 INTERPRETING THE LOCAL ADF

The solar neighbourhood ADF has been subject to previous investigation. In particular, Lamers et al. (2005) and Lamers & Gieles (2006) employed the cluster dissolution processes 1–4 (Section 3) to study the ADF of 114 OCs closer than $d_{\odot} = 0.6$ kpc taken from Kharchenko et al. (2005). Their ADF can be reasonably well described by a nearly-constant [in bound clusters of mass $10^2 < M(\mathrm{M}_{\odot}) < 3\times10^4$] SFR $= 400\,\mathrm{M}_{\odot}\,\mathrm{Myr}^{-1}$, corresponding to a surface SFR $\Sigma_{\mathrm{SFR}} \approx 350\,\mathrm{M}_{\odot}\,\mathrm{Myr}^{-1}\,\mathrm{kpc}^{-2}$, which is considerably lower than $\Sigma_{\mathrm{SFR}} = 700$–$1000\,\mathrm{M}_{\odot}\,\mathrm{Myr}^{-1}\,\mathrm{kpc}^{-2}$ inferred from ECs (Lada & Lada 2003) and $\Sigma_{\mathrm{SFR}} = 3000$–$7000\,\mathrm{M}_{\odot}\,\mathrm{Myr}^{-1}\,\mathrm{kpc}^{-2}$ implied by field stars (Miller & Scalo 1979). They also find evidence of a local burst of star formation that took place between 250 and 600 Myr ago (also present in Piskunov et al. 2006).

Besides cluster dissolution, observational completeness is also important for the ADF shape. High absorption and crowding, usually associated with fields dominated by disc and bulge stars, affect cluster detectability, especially the faint and/or poorly populated ones. Bonatto et al. (2006) show that most of the intrinsically faint and/or distant clusters must be undetected in the field, particularly in bulge/disc directions. They also find that the completeness-safe zone might extend up to $d_{\odot} \approx 1.4$ kpc inside the solar circle, but considerably more outside.

Thus, to minimize observational completeness effects, we restrict the analysis to the region $d_{\odot} \leq 1$ kpc, which reduces the number of clusters to 442, but still a statistically significant sample. Besides, this condition also guarantees that we are dealing with clusters subject to somewhat similar physical conditions. By construction (Section 2), the resulting ADF (Fig. 1) is rather smooth, with small errors over all ages, except for $t_{\mathrm{A}} \gtrsim 3$ Gyr, which reflects the scarcity of Gyr-old clusters in the region. Also conspicuous are the excesses between $200 \lesssim t_{\mathrm{A}}(\mathrm{Myr}) \lesssim 600$, and especially for $t_{\mathrm{A}} \lesssim 10$ Myr (see below). Since we work with a significantly larger sample than Lamers et al. (2005) and Lamers & Gieles (2006), our approach provides a better definition of structures in the ADF.

4.1 ADF simulation

Instead of assuming particular values for the several model parameters (R_{GC}, W_0, γ, t_R, ϵ, number, age, initial mass and the orbit of clusters), we adopt a simplifying approach. Starting with a predefined SFR, we compute the time-evolution of the individual mass of star clusters created with parameters covering the observed range in orbits around the solar circle (Lamers et al. 2010). We assume that the relevant model parameters can take on any value within $0.0 \leq \epsilon \leq 0.8$ (also allowing for circular orbits), $5 \leq W_0 \leq 7$, $0.65 \leq \gamma \leq 0.8$ and $3.5 \leq t_R(\mathrm{Myr}) \leq 13.3$ (the latter two are expressed as a function of W_0 as $t_R = 37.8 - 4.9W_0$ and $\gamma = 0.275 + 0.075W_0$); also, given the restriction $d_{\odot} \leq 1$ kpc, we have $7.5 \leq R_{\mathrm{GC}}(\mathrm{kpc}) \leq 9.5$. Each cluster is created (at time t_{A}) with an individual mass in the range $M_{\mathrm{min}} < M_{\mathrm{i}}(\mathrm{M}_{\odot}) < M_{\mathrm{max}}$, but following the number-frequency (or probability) $\mathrm{d}N/\mathrm{d}M_{\mathrm{i}} \propto M_{\mathrm{i}}^{-2}$ (e.g. Elmegreen 2008).[6]

[6] This is done by considering $M_{\mathrm{i}} = \frac{M_{\mathrm{min}}}{1-n(1-M_{\mathrm{min}}/M_{\mathrm{max}})}$, where n is uniformly distributed within [0,1].

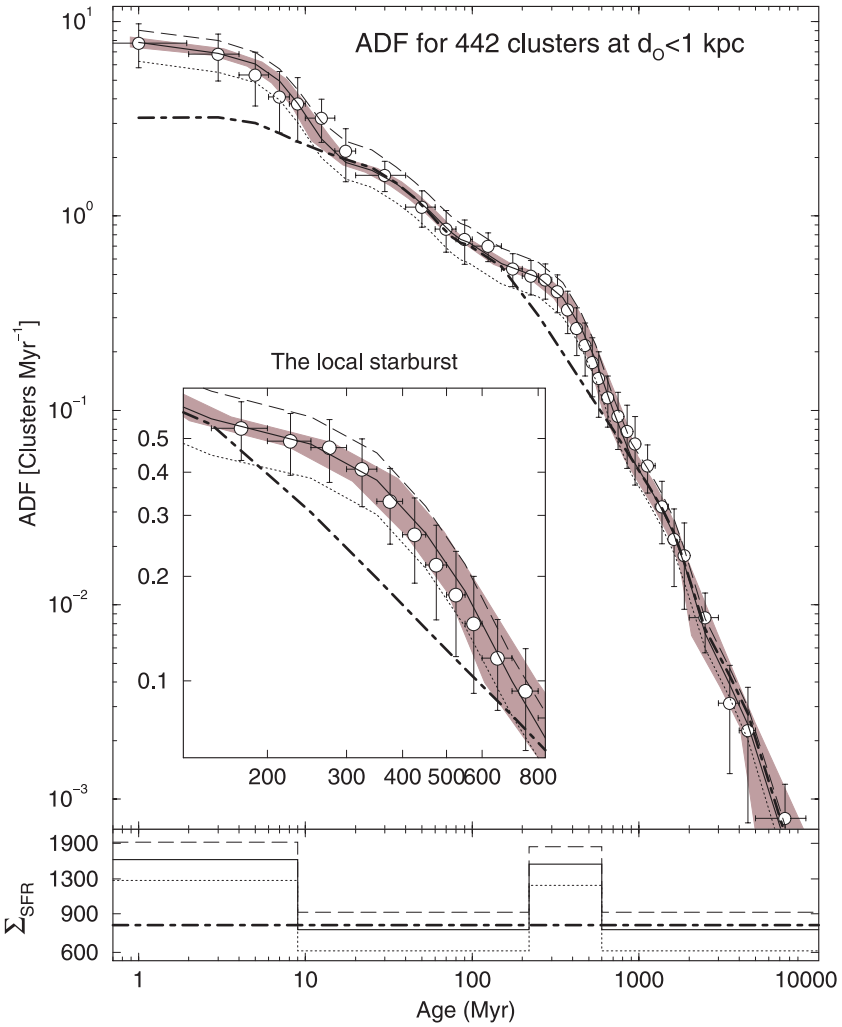

Figure 1. Top panel: the solar neighbourhood ADF (circles) is well reproduced by a segmented SFR (thick solid line) with enhanced rates at $\lesssim$9 Myr and 220–600 Myr and small stochastic fluctuations over 100 simulations (shaded region). Also shown are the ADFs produced by $\Sigma_{\rm SFR}$ 20 per cent higher (dashed line) and lower (dotted line) than above, together with that produced by constant $\Sigma_{\rm SFR}$ (thick dot–dashed line). Inset: blow-up of the local starburst period. Bottom panel: $\Sigma_{\rm SFR}$ (in $\rm M_\odot\,Myr^{-1}\,kpc^{-2}$) used in the top panel.

We adopt $M_{\rm min} = 10\,\rm M_\odot$ and $M_{\rm max} = 7.5 \times 10^4\,\rm M_\odot$ as the minimum and maximum initial cluster masses, respectively. Then, we solve equation (1) to find the mass remaining in each cluster after evolving for a time from $t = 0$ to $t_{\rm A}$, and build the simulated ADF. Similarly to Lamers & Gieles (2006), we assume $100\,\rm M_\odot$ as the minimum cluster mass for completeness not being an issue to detectability, that is, only clusters more massive than $100\,\rm M_\odot$ are accounted for in the ADF. According to this approach, the number of free parameters reduces essentially to the SFR shape.

The following steps are taken. (i) We assume that all star formation occurs in clusters, define the SFR and compute the total mass [$M_{\rm tot} = \int {\rm SFR}(t)\,{\rm d}t$] converted into stars over the Galaxy age; in the case of a non-constant SFR, this should be done separately for each SFR segment (or period of time). (ii) We assign the initial mass $M_{\rm i}$ (see above) for one cluster. (iii) Next, we randomly assign the cluster age $t_{\rm A}$ (it should be within the corresponding SFR time-segment) and the model parameters. (iv) Steps (ii) and (iii) are repeated for more clusters, until the sum of the initial masses equals $M_{\rm tot}$. (v) Then, we solve equation (1) for all clusters from $t = 0$ to $t_{\rm A}$ and keep only those with $M(t_{\rm A}) > 100\,\rm M_\odot$. (vi) Finally, stochastic effects are minimized by repeating steps (ii)–(v) several times ($N_{\rm sim}$). In the present case, we use $N_{\rm sim} = 100$ and solve equation (1) for $M = M(t)$ by means of a fourth-order Runge–Kutta method, with a fixed time-step of 1 Myr.

4.2 Constraining the local SFR

Given the conspicuous excesses (Fig. 1), it is clear that the solar neighbourhood cluster ADF cannot result from a constant SFR. Instead, the best match has been obtained with the segmented SFR: ${\rm SFR} = 5040\,\rm M_\odot\,Myr^{-1}$ ($\Sigma_{\rm SFR} \approx 1600\,\rm M_\odot\,Myr^{-1}\,kpc^{-2}$) for $t_{\rm A} \leq 9$ Myr; ${\rm SFR} = 4800\,\rm M_\odot\,Myr^{-1}$ ($\Sigma_{\rm SFR} \approx 1500\,\rm M_\odot\,Myr^{-1}\,kpc^{-2}$) for $220 \leq t_{\rm A}({\rm Myr}) \leq 600$; and ${\rm SFR} = 2400\,\rm M_\odot\,Myr^{-1}$ ($\Sigma_{\rm SFR} \approx 760\,\rm M_\odot\,Myr^{-1}\,kpc^{-2}$) elsewhere (bottom panel of Fig. 1). Integrating the segmented-SFR ADF over time yields the same number of clusters as that of the observed ADF. Also, the 1σ boundaries of the adopted solution (shaded region in Fig. 1), obtained after 100 different simulations, are very narrow over most of the cluster ages. To check how constrained is this solution, we apply the same procedure to SFRs that are 20 per cent higher and lower than the adopted SFR over all time periods. Overall, both SFRs provide a much poorer description of the observed ADF than the segmented

SFR, especially for clusters younger than ∼300 Myr. Thus, we adopt 20 per cent as the SFR uncertainty. As expected, the ADF produced by a constant SFR (2500 $M_\odot$ Myr^{-1}) fails to describe the observed excesses.

Considering the above arguments, the average values (over the full age range) of the SFR and surface SFR are $\overline{SFR} \approx (2500 \pm 500)\,M_\odot\,Myr^{-1}$ and $\overline{\Sigma}_{SFR} \approx (790 \pm 160)\,M_\odot\,Myr^{-1}\,kpc^{-2}$, respectively. Given the higher number of clusters in our sample, we find Σ_{SFR} more than twice that of Lamers et al. (2005) and Lamers & Gieles (2006), considerably more consistent with that inferred from ECs by Lada & Lada (2003), but still significantly lower (∼16 per cent) than the rate implied by field stars (Miller & Scalo 1979). We also compute the fraction of clusters that do not survive the first 10 Myr, 91.2 ± 2.7 per cent, which agrees with the rate of cluster dissolution after the embedded phase (e.g. Lada & Lada 2003).

On average, $\sim 3.3 \times 10^5$ clusters are created (at $d_\odot < 1$ kpc) in each simulation with the segmented SFR. This implies that less than 0.15 per cent of the clusters ever formed in the solar neighbourhood can be observed (i.e. having mass $\gtrsim 100\,M_\odot$) and, if the same SFR applies to $R_{GC} = 7.5$–9.5 kpc, $\sim 10^7$ clusters have been created in this region since the Galaxy formation.

5 SUMMARY AND CONCLUSIONS

In this paper, we analyse properties of the solar neighbourhood SFR, by means of a statistically significant ADF built with 442 star clusters (ECs and OCs) closer than 1 kpc from the Sun. By adopting a simplifying approach, in which the mass evolution of artificial clusters is followed over time, we reduce the problem to essentially finding the SFR.

The artificial clusters embody parameters and conditions expected to apply to most actual star clusters orbiting not far from the solar circle. To simulate the observed ADF, we employ semianalytical descriptions of the mass-loss process responsible for cluster dissolution and assume that only clusters with a present-day mass above 100 $M_\odot$ can be effectively observed (i.e. take part in the ADF).

The best match between observed and simulated ADFs corresponds to a non-constant SFR, with enhanced rates for the ages ≤9 Myr and 220–600 Myr (the so-called local starburst). The average SFR is $\overline{SFR} \approx (2500 \pm 500)\,M_\odot\,Myr^{-1}$, corresponding to the average density $\overline{\Sigma}_{SFR} \approx (790 \pm 160)\,M_\odot\,Myr^{-1}\,kpc^{-2}$. These values agree with the SFR inferred from ECs, but represent only ∼16 per cent of the rate implied by field stars. Both the local starburst and the recent formation (≤9 Myr) have ADF amplitudes suggesting periods with a SFR about twice the average value. We also find that 91.2 ± 2.7 per cent of the clusters created in the solar neighbourhood dissolve before 10 Myr, which is consistent with the rate of EC dissolution.

ACKNOWLEDGMENTS

We thank the referee, Simon Portegies Zwart, for the comments. We acknowledge the support from the Brazilian Institution CNPq. This publication makes use of the WEBDA data base, operated at the Institute for Astronomy of the University of Vienna.

REFERENCES

Anders P., Fritze-v.Alvensleben U., 2003, A&A, 401, 1063
Baumgardt H., Makino J., 2003, MNRAS, 340, 227
Benjamin R. A. et al., 2003, PASP, 115, 953
Bica E., Dutra C. M., Soares J., Barbuy B., 2003, A&A, 404, 223
Bonatto C., Santos J. F. C., Jr, Bica E., 2006, A&A, 445, 567
Bonatto C., Kerber L. O., Bica E., Santiago B. X., 2006, A&A, 446, 121
Bonatto C., Bica E., 2007, A&A, 473, 445
Bonatto C., Bica E., 2008, A&A, 491, 767
Bonatto C., Bica E., 2009a, MNRAS, 392, 483
Bonatto C., Bica E., 2009b, MNRAS, 394, 2127
Bonatto C., Bica E., 2009c, MNRAS, 397, 1915
Bonatto C., Bica E., 2010a, A&A, 516, 81
Bonatto C., Bica E., 2010b, A&A, 521A, 74
Dias W. S., Alessi B. S., Moitinho A., Lépine J. R. D., 2002, A&A 389, 871
Dutra C. M., Bica E., Soares J., Barbuy B., 2003, A&A, 400, 533
Efremov Yu. N., 1995, AJ, 110, 2757
Elmegreen B. G., 2008, Globular Clusters - Guides to Galaxies, ESO Astrophysics Symposia. Springer-Verlag, Berlin, Heidelberg
Froebrich D., Scholz A., Raftery C. L., 2007, MNRAS, 374, 399
Froebrich D., Schmeja S., Samuel D., Lucas P. W., 2010, MNRAS, 409, 1281
Gieles M., Baumgardt H., 2008, MNRAS, 389, 28
Gieles M., Athanassoula E., Portegies Zwart S. F., 2007, MNRAS, 376, 809
Goodwin S. P., Bastian N., 2006, MNRAS, 373, 752
Khalisi E., Amaro-Seoane P., Spurzem R., 2007, MNRAS, 374, 703
Kharchenko N. V., Piskunov A. E., Röser S., Schilbach E., Scholz R.-D., 2005, A&A, 438, 1163
Kumar M. S. N., Kamath U. S., Davis C. J., 2004, MNRAS, 353, 1025
Kumar M. S. N., Keto E., Clerkin E., 2006, A&A, 449, 1033
Lada C. J., Lada E. A., 2003, ARA&A, 41, 57
Lamers H. J. G. L. M., Gieles M., 2006, A&A, 455, L17
Lamers H. J. G. L. M., Gieles M., Bastian N., Baumgardt H., Kharchenko N. V., Portegies Zwart S., 2005, A&A, 441, 117
Lamers H. J. G. L. M., Baumgardt H., Gieles M., 2010, MNRAS, 409, 305
Larsen S., 2004, A&A, 416, 537
Miller G. E., Scalo J. M., 1979, ApJS, 41, 513
Ortolani S., Bonatto C., Bica E., Momany Y., Barbuy B., 2008, New Astron., 13, 508
Piskunov A. E., Kharchenko N. V., Röser S., Schilbach E., Scholz R.-D., 2005, A&A, 445, 545
Salpeter E. E., 1955, ApJ, 121, 161
Skrutskie M. F. et al., 2006, AJ, 131, 1163
Spitzer L., 1987, Dynamical Evolution of Globular Clusters. Princeton Univ. Press, Princeton, NJ

This paper has been typeset from a TEX/LATEX file prepared by the author.